South Eastern Australian
Climate initiative

Final report for Project 2.1.4

Evaluation of statistically downscaled projections

Principal Investigator:
Steve Charles
Steve.Charles@csiro.au

Co-Author:
Guobin Fu

CSIRO Land and Water
Ph: 02 6246 5617
seaci@csiro.au
http://www.seaci.org

Australian Government
Department of Climate Change
Bureau of Meteorology

MURRAY–DARLING BASIN AUTHORITY

State Government Victoria
Department of Sustainability and Environment

National Research FLAGSHIPS
Water for a Healthy Country
CSIRO

Abstract

An ensemble of stochastic daily rainfall projections has been investigated. The ensemble was generated using the Nonhomogeneous hidden Markov model (NHMM) downscaling model and driven by atmospheric predictors from four global climate models (GCMs) (for three emissions scenarios and two periods). The aim has been to see what changes in regional rainfall come about as a result of using particular GCMs, scenarios, and periods.

Significant research highlights, breakthroughs, and snapshots

- Climate change projections of daily rainfall for 30 stations in the lower Murray–Darling Basin have been produced, and these are suitable for assessing the hydrological impact of changes in rainfall timing, frequency, and intensity.

- For a number of hydrologically relevant metrics, we see an overall consistency in the projected changes. The projections indicate a decrease in total rainfall, particularly in winter (April–October), an increase in daily maximum rainfall, a decrease in less extreme daily rainfall (e.g. 95th and 90th percentile), a decrease in the number of rainfall events, and an increase in the length of runs of consecutive dry days.

- By mid-century (2046–2065), there is considerable overlap in the projections obtained from the three emissions scenarios. In contrast, by the end of the century (2081–2100) the projections have diverged, with the changes in rainfall proportional to the relative strengths of the respective scenarios. This suggests that global mitigation efforts would reduce the magnitude of future rainfall changes over the study region.
- Uncertainties in the range of projected changes are dominated by differences between the projections obtained from the four GCMs. This suggests the continuing need for GCM improvement and for better assessment and selection of which GCMs can be used with confidence.

Statement of results, their interpretation, and practical significance against each objective

Objective 1: Assess hydrologically relevant properties of weather state and multi-site rainfall projections obtained from stochastically-downscaled GCM runs for selected scenarios and periods.

The changes in NHMM downscaled weather-state sequences are driven by the changes in atmospheric predictors projected by the GCM scenarios. The projected multi-site daily rainfall series are conditional on these weather-state sequence changes, and thus in turn the predictor changes. Tables 1 and 2 summarise projected weather-state frequency changes, using the Mk3.5 projections as an example (see Appendix A for the other GCMs). The first number in each cell is the mean probability of occurrence (i.e. frequency) of the weather state for the given downscaled scenario. The second number, in brackets, is the number of 'standard errors' between this probability and the baseline 20th century downscaled weather-state probability (20C3M). It is thus a measure of the relative significance of the projected change in weather-state frequency. [Note: plots of the weather states are presented in Appendix A of the Project 1.5.2 & 3 report].

There is strong consistency in the *direction* of the state changes across virtually all the scenarios and periods. The dry State 1 increases in frequency for all scenarios and periods for both summer and winter, and the wet State 2, likewise, decreases.

There is also a consistent response in the *magnitude* of the state changes to the different emissions scenarios by the end of the century, corresponding to the relative strength of each scenario. Thus the relatively high emission A2 produces the largest changes for all weather states for both summer and winter. The response is more mixed for mid-century, given that by then greenhouse gas concentrations have not significantly diverged between the scenarios. The B1 scenario has a low emission trajectory, so greenhouse gas concentration growth between mid (2046–2065) and late (2081–2100) century is small compared to the other two scenarios investigated. As a result, for several states the B1 end-of-century change is less than the mid-century change. Some mid-century changes are also greater than the end-of-century changes for the two higher emission scenarios (e.g. winter State 4). In both cases this indicates the potential for projected changes to be as responsive to interdecadal climate variability as they are to long-term climate change.

The downscaled projections for annual rainfall, averaged across the 30 stations, indicate a decrease for both the 2046–2065 and 2081–2100 periods for all scenarios and climate models (Figure 1), except for a slight increase for CCAM for the A2 scenario in 2081–2100.

Table 1. Summer Mk3.5 downscaled weather-state mean frequencies (and standard errors, in brackets, relative to 20C3M)

State	20C3M	A1B mid*	A1B end*	A2 mid	A2 end	B1 mid	B1 end
1	0.525	0.556 (1.67)	0.565 (1.95)	0.573 (2.21)	0.578 (2.75)	0.569 (2.05)	0.533 (0.41)
2	0.083	0.068 (1.49)	0.055 (3.07)	0.058 (2.67)	0.051 (3.73)	0.058 (2.80)	0.070 (1.46)
3	0.100	0.095 (0.73)	0.089 (1.72)	0.084 (2.11)	0.085 (2.32)	0.087 (2.04)	0.099 (0.19)
4	0.055	0.063 (2.81)	0.064 (3.22)	0.062 (2.13)	0.068 (4.17)	0.062 (2.35)	0.062 (3.09)
5	0.237	0.218 (2.12)	0.227 (0.92)	0.223 (1.30)	0.219 (1.74)	0.224 (1.08)	0.236 (0.06)

* 'mid' refers to the 2046–2065 period; 'end' refers to the 2081–2100 period

Table 2. Winter Mk3.5 downscaled weather-state mean frequencies (and standard errors, in brackets, relative to 20C3M)

State	20C3M	A1B mid	A1B end	A2 mid	A2 end	B1 mid	B1 end
1	0.439	0.512 (3.45)	0.550 (5.26)	0.495 (2.60)	0.562 (6.09)	0.488 (2.40)	0.513 (3.89)
2	0.117	0.089 (2.81)	0.067 (4.95)	0.093 (2.09)	0.063 (5.74)	0.091 (2.61)	0.087 (2.87)
3	0.098	0.083 (2.48)	0.071 (4.22)	0.085 (2.08)	0.069 (4.50)	0.087 (1.51)	0.083 (2.55)
4	0.206	0.200 (0.65)	0.201 (0.45)	0.214 (1.11)	0.199 (0.79)	0.208 (0.24)	0.208 (0.23)
5	0.140	0.116 (2.64)	0.111 (3.53)	0.113 (3.11)	0.107 (4.06)	0.126 (1.49)	0.108 (3.59)

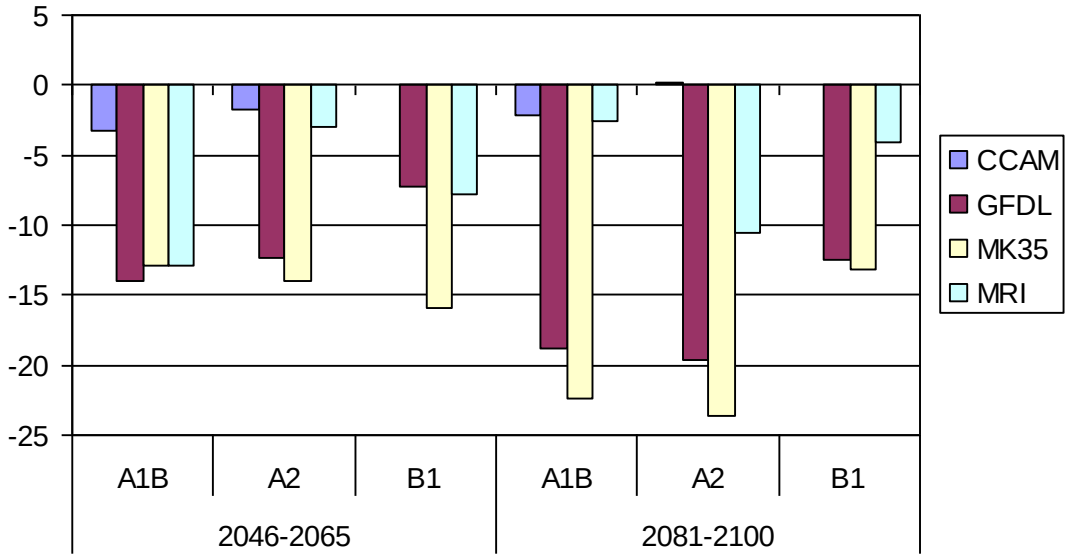

Figure 1. Annual rainfall change (%).

Two climate models (GFDL and Mk3.5) consistently project a decline in summer (Nov–Mar) rainfall, and two (CCAM and MRI) indicate an increase in summer rainfall (Figure 2). This is interesting considering that the CCAM model is nudged by the Mk3.0 atmosphere and uses the Mk3.0 sea-surface temperatures as the ocean boundary condition. In contrast, all four climate models show a decrease in winter (Apr–Oct) rainfall (Figure 3). Since winter rainfall accounts for two-thirds of the annual rainfall and produces the majority of streamflow for this region, this decrease in winter rainfall would cause additional water-availability concerns in the south-eastern corner of the Murray–Darling Basin, especially since water shortages are already producing a critical problem in the region.

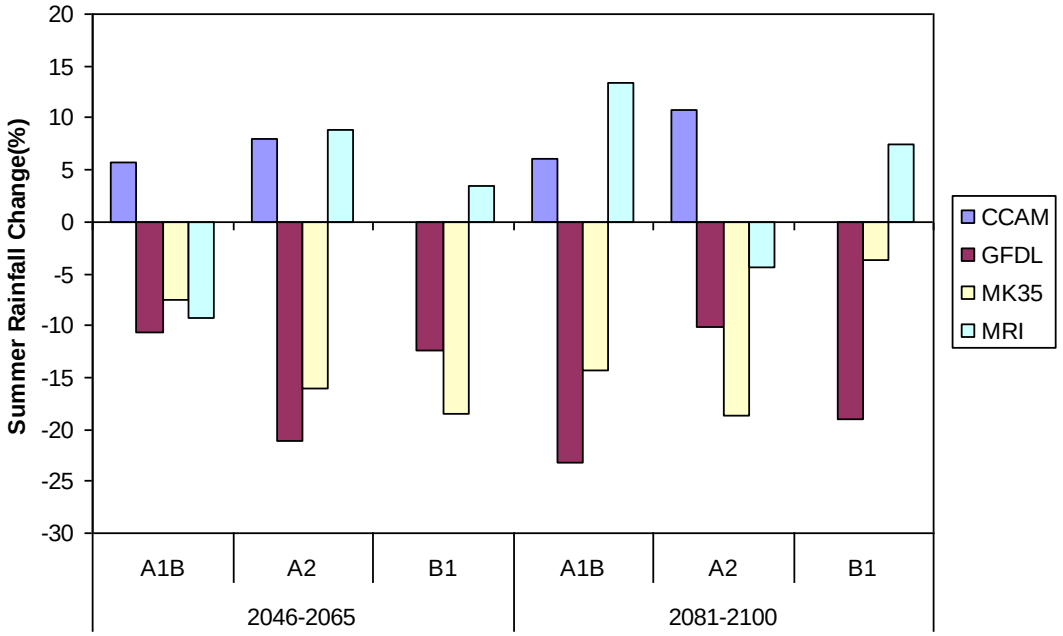

Figure 2. Summer rainfall change (%).

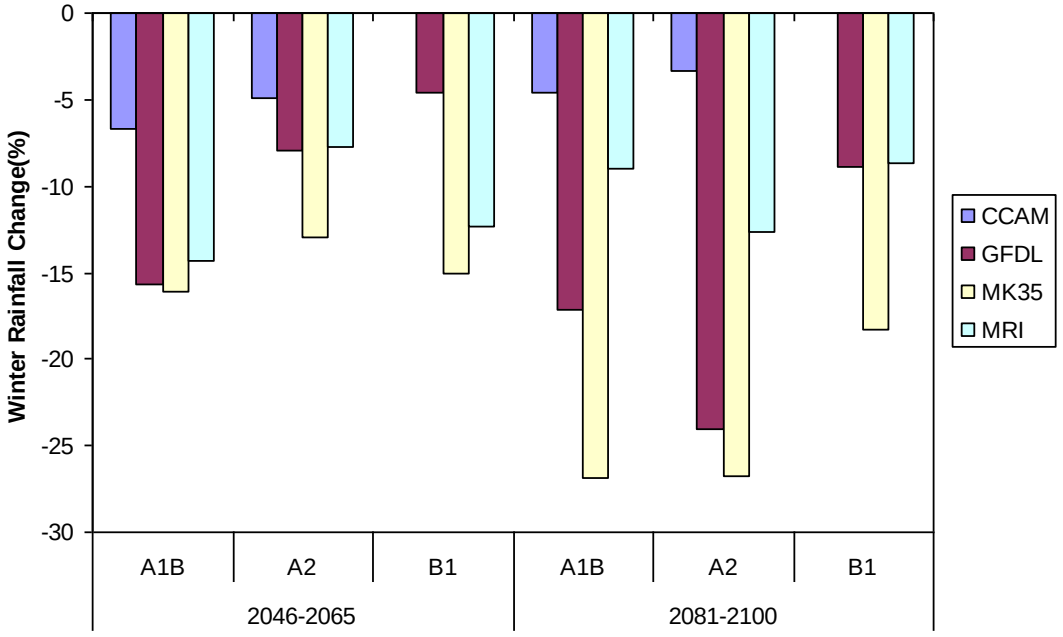

Figure 3. Winter rainfall change (%).

The 2046–2065 monthly distribution of projected changes indicates a January and February rainfall increase and an April–October rainfall decline (Figure 4). However, there are inconsistencies between the GCMs. For example, three GCMs (GFDL, Mk3.5, and MRI) project a monthly rainfall decline for December, but CCAM projects an increase for this month for the 2046–2065 period.

The decreasing rainfall trend for April–October is more significant for the period 2081–2100 than 2046–2065 (Figure 5). It implies that the change becomes larger as atmospheric gas emissions accumulate.

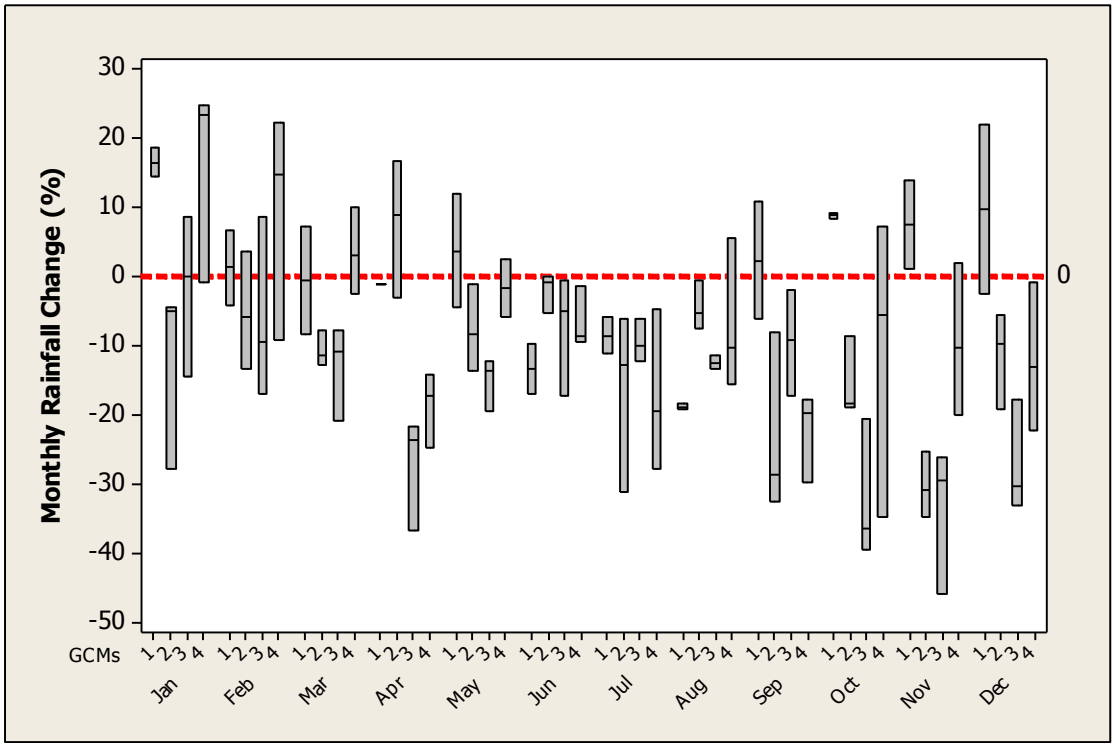

Figure 4. Monthly rainfall change (%) for 2046–2065 vs 1961–2000.

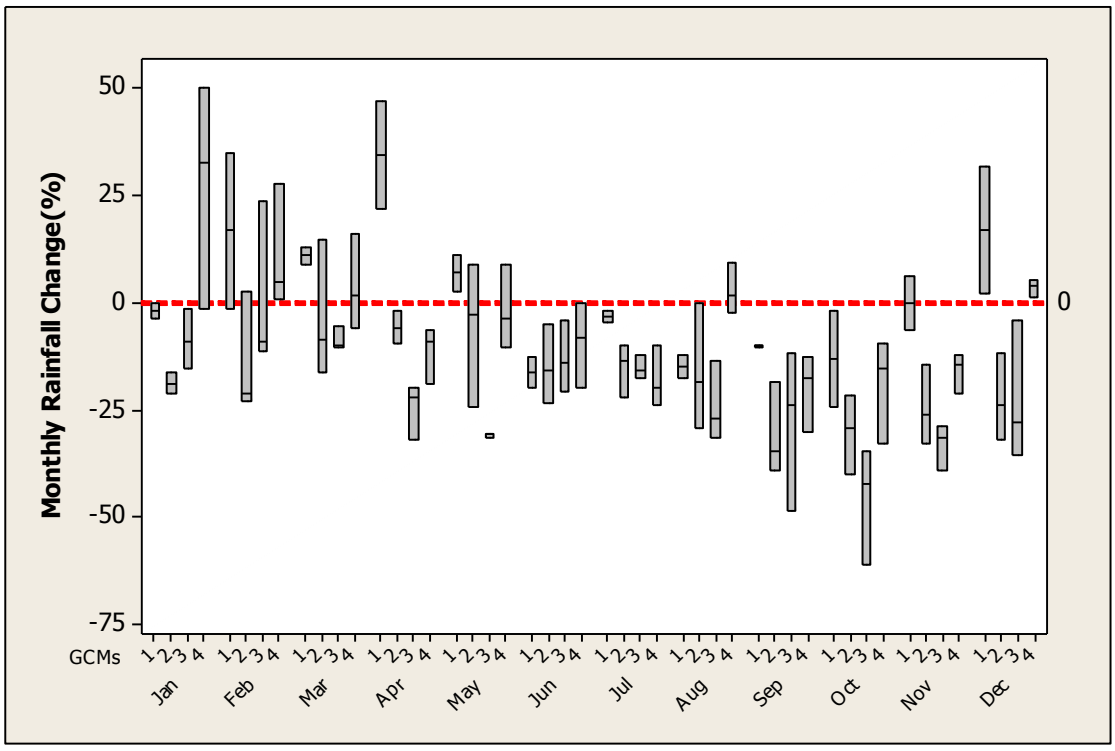

Figure 5. Monthly rainfall change (%) for 2081–2100 vs 1961–2000.

The annual maximum daily rainfall is projected to intensify in the future, particularly by the end of the century (Figure 6). This result implies a potential for a slight increase in the probability of intense floods in the study region.

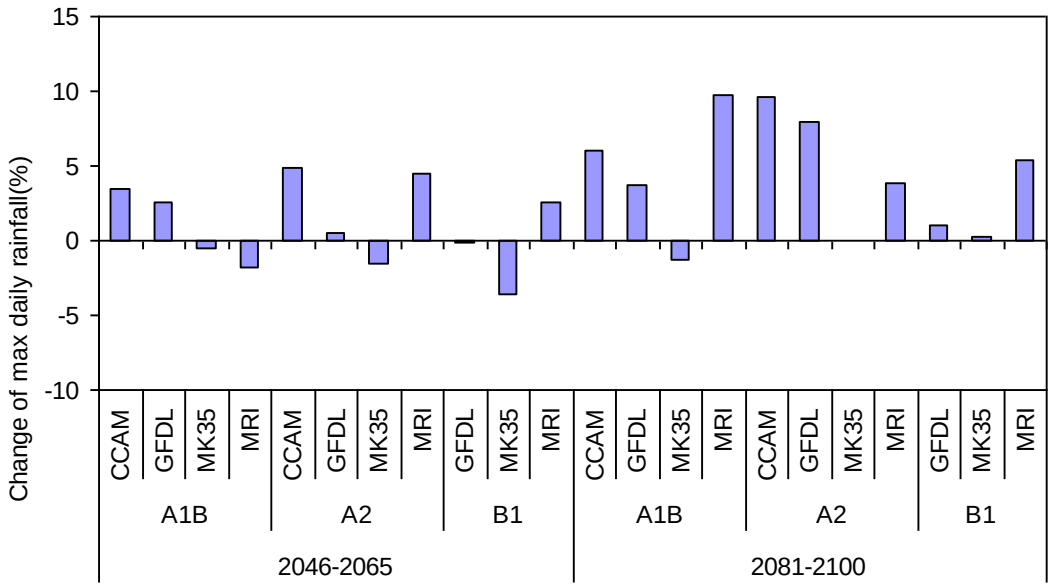

Figure 6. Changes in annual maximum daily rainfall (%).

The 99th percentile of daily rainfall does not have as significant a trend as daily maximum rainfall (Figure 7). The changes are smaller than those of maximum daily rainfall, and there are more climate models and scenarios indicating a decreasing trend.

The 95th and 90th percentiles of daily rainfall, in contrast, are projected to decrease in the future, especially for the 2081–2100 period (Figures 8 and 9). This conclusion is consistent with the majority of recent climate-change modelling literature, where projections of increased extremes alongside decreasing means are common (IPCC 2007, and references therein).

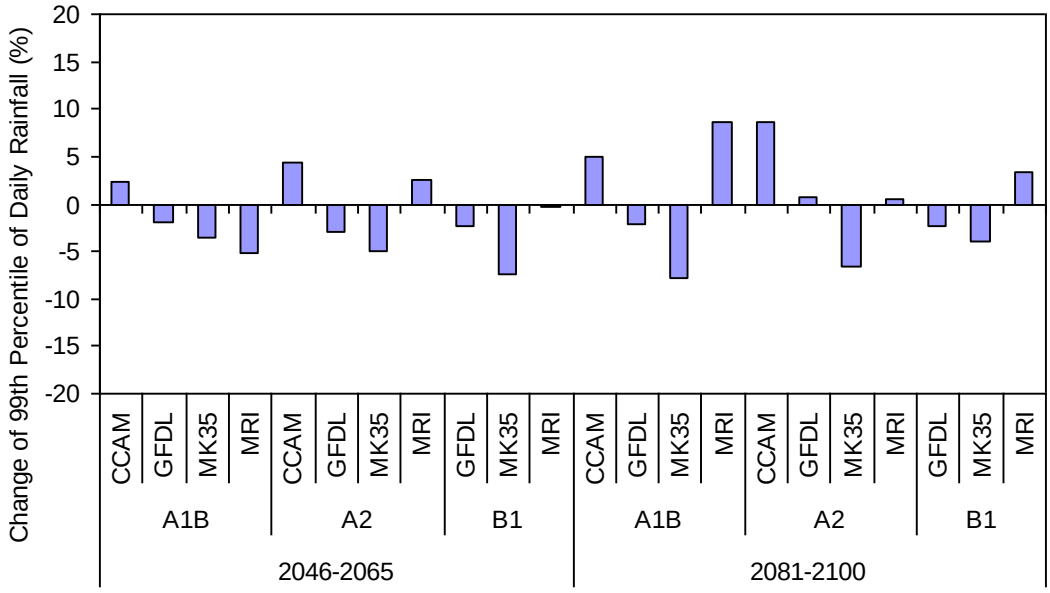

Figure 7. Changes in 99th percentile of daily rainfall (%).

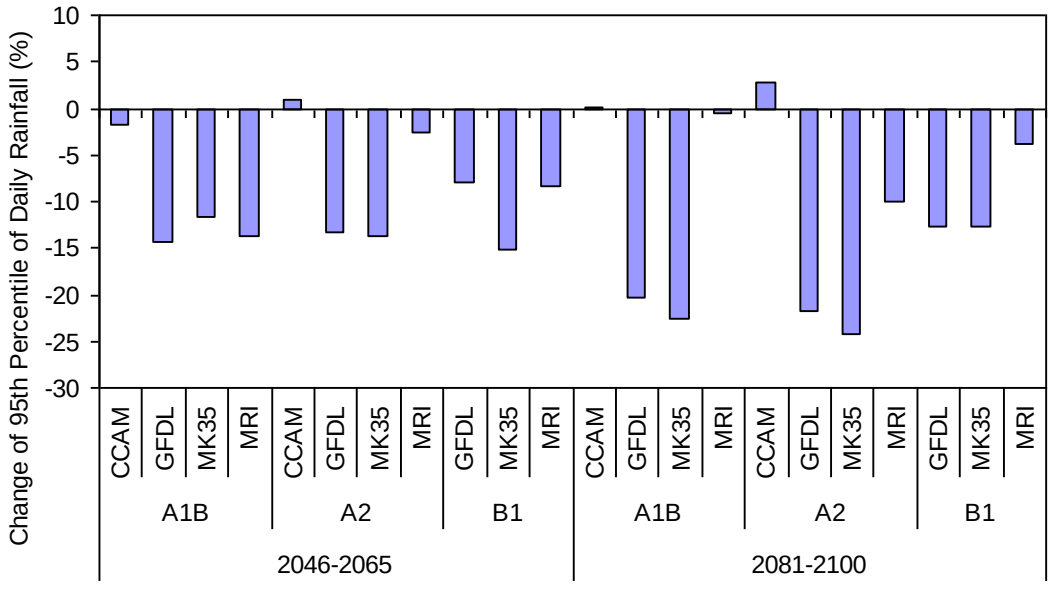

Figure 8. Changes in 95th percentile of daily rainfall (%).

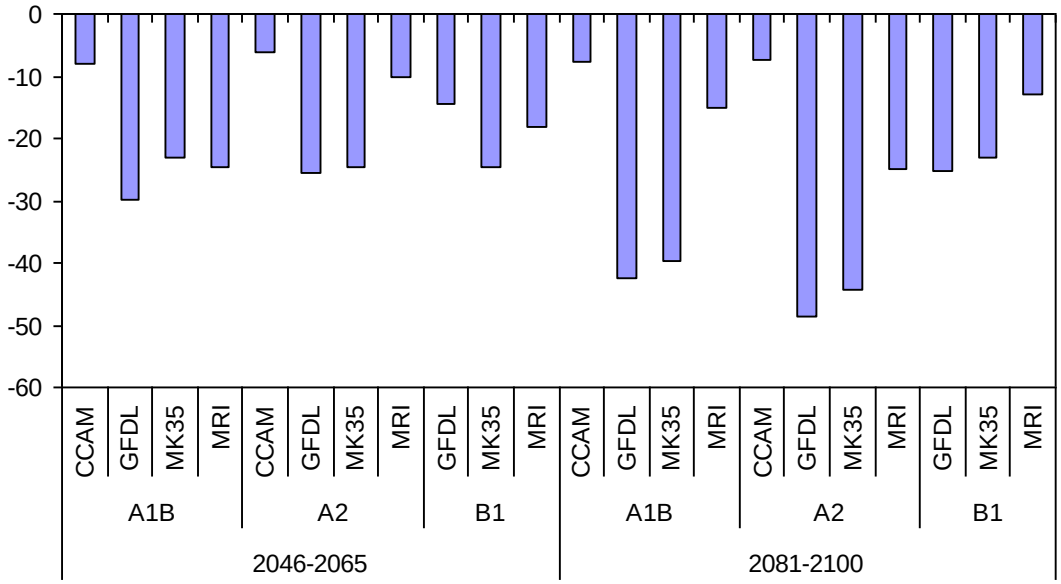

Figure 9. Changes in 90th percentile of daily rainfall (%).

The number of dry days would increase (Figure 10) and wet days decrease (Figure 11), a result consistent across all climate models and emission scenarios. This conclusion is in line with analysis of GCM projections by Pitman and Perkins (2008). Together with the projected decrease in annual rainfall and an increase in maximum daily rainfall, this would lead to decreased runoff and streamflow, suggesting more severe water-availability problems for the study region.

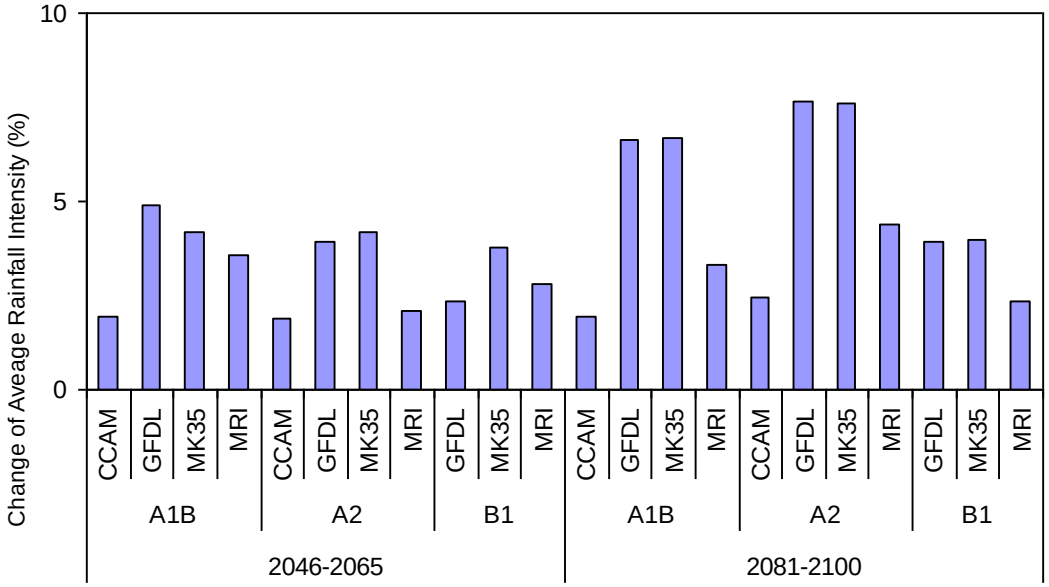

Figure 10. Change in dry day occurrence (%).

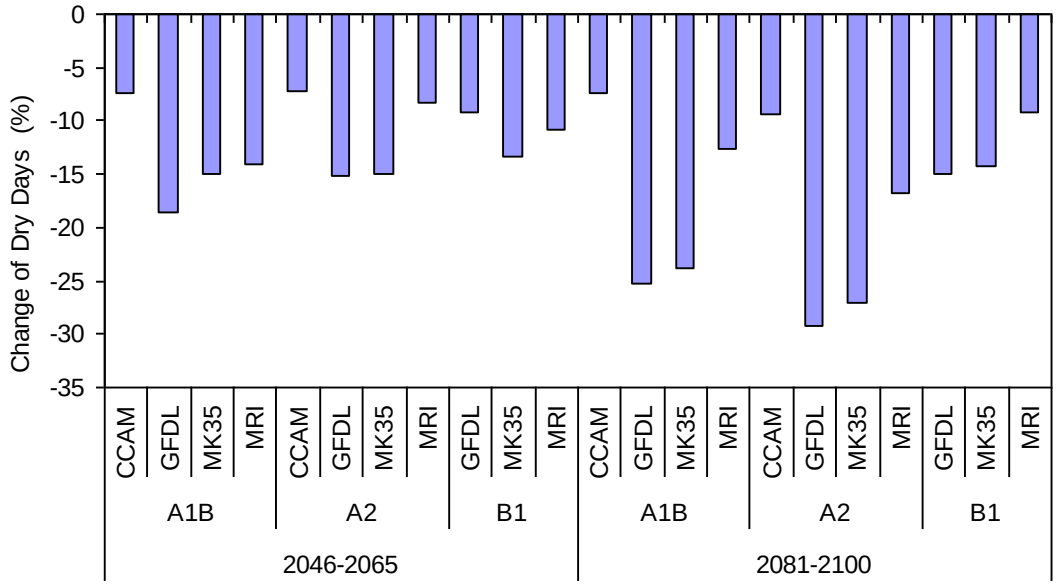

Figure 11. Change in wet day occurrence (%).

The maximum length of consecutive dry days is also projected to increase (Figure 12). This change would also have implications for runoff and streamflow, and hence water availability. Correspondingly, there is a consistent projection of the maximum length of consecutive wet days decreasing (Figure 13). This change in daily sequencing, combined with fewer events with reduced amounts, would lead to drier catchment soil profiles and would further reduce runoff.

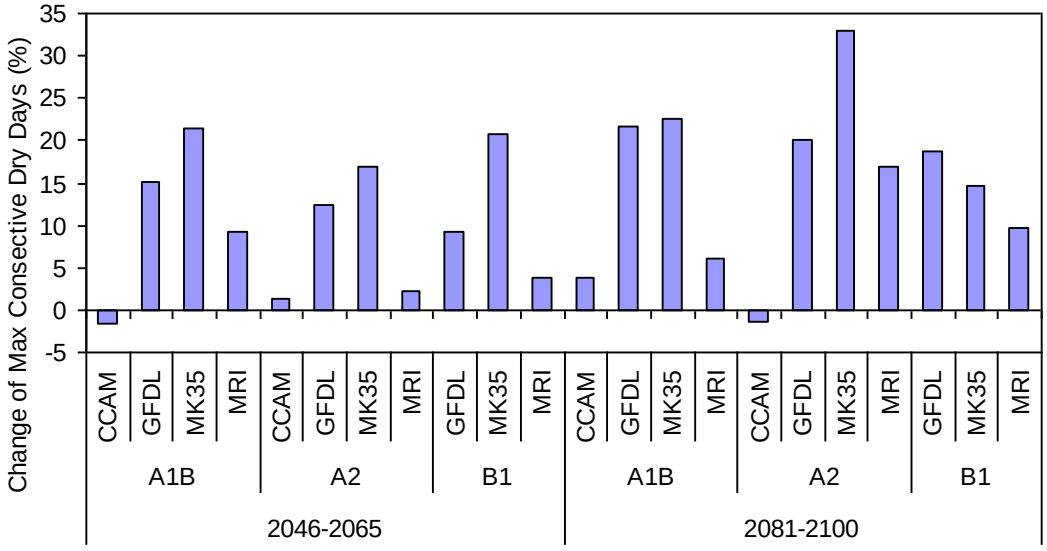

Figure 12. Changes of maximum consecutive dry days (%).

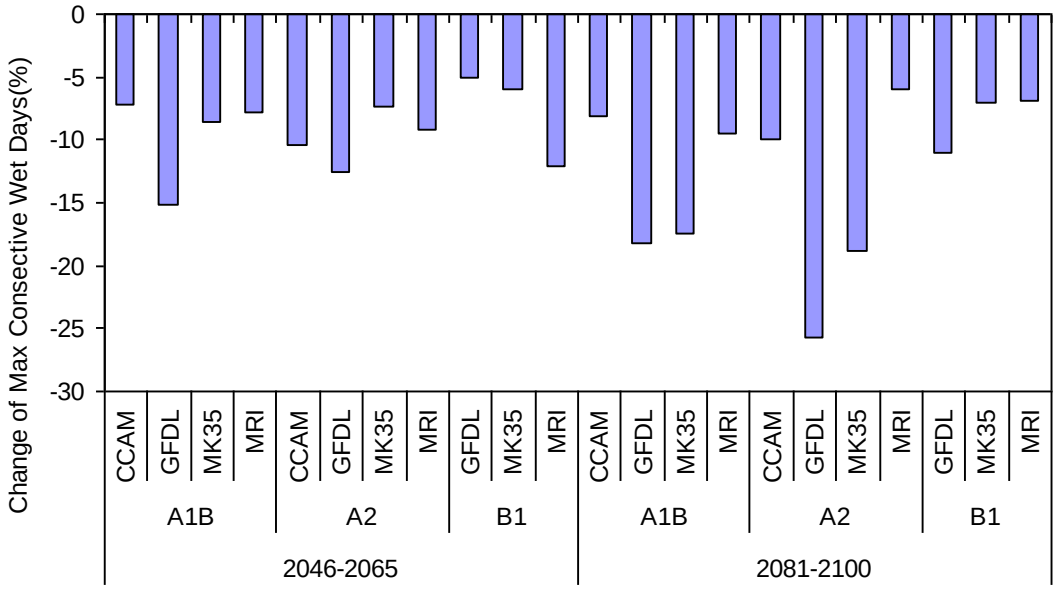

Figure 13. Changes of maximum consecutive wet days (%).

Objective 2: Compare these properties for transient and stabilised periods in the emissions scenarios.

Detailed analysis of stabilised period projections has not been undertaken. It was originally envisaged that long stabilised runs would be analysed for return periods of extended dry and wet events (e.g. multi-year droughts). However only one GCM, Mk3.5, has such long runs available and so no comparison or assessment of a range of responses was possible. This aspect of downscaled projections may be looked at in future work.

Objective 3: Assess the consistency, range, and relative sources of uncertainty in the projected changes to the hydrologically relevant metrics.

The results presented for the two periods for the different GCM and emission scenarios highlight the consistencies and the relative contribution to uncertainty between the GCMs, scenarios, and periods. In common with other studies (e.g. Fowler et al. 2007, Kay et al. 2009), the differences between the GCMs produce the greatest source of uncertainty. Appendix B, Table B1, presents a summary of the range of uncertainty by station, highlighting the large between-GCM ranges and smaller between-scenario ranges. The projected rainfall changes for individual stations also highlight that the range in uncertainty increases with time (end-of-century projections compared to the mid-century) and with the intensity of the emissions scenario (i.e. for mid-century there are lower between-scenario uncertainties). These results are summarised, averaging across the 30 stations, in Table 3. Using an example for 2046–2065, the mean range in projected annual rainfall change across the three scenarios for the Mk3.5 was 3.4 per cent, whereas the mean range across the four GCMs for A2 was 14.2 per cent. The

maximum range for an individual station is 30.7 per cent across the GCMs for the A2 scenario in 2081–2100.

Table 3. Range (%), by GCM and emissions scenario, of 30-station minimum, maximum, and mean projected annual rainfall change

	2046–2065						
	B1*	A1B	A2	CCAM*	GFDL	Mk3.5	MRI
Min	6.5	9.0	7.6	0.3	2.1	0.6	5.7
Max	13.9	15.8	21.3	4.3	10.6	6.6	13.7
Mean	9.9	12.0	14.2	2.1	6.5	3.4	10.6
	2081–2100						
	B1*	A1B	A2	CCAM*	GFDL	Mk3.5	MRI
Min	6.7	17.7	18.7	0.4	3.7	7.3	5.3
Max	14.4	28.6	30.7	7.2	11.3	13.1	13.6
Mean	9.9	22.6	25.8	2.8	7.1	10.2	9.1

* Note B1 is the range across only three GCMs and CCAM is the range across only two scenarios, A1B and A2, due to the unavailability of a CCAM B1 scenario

The pervasive impact of GCM bias, which varies across the GCMs, on our confidence in these projections cannot be ignored. The magnitude of GCM bias for current climate for the SEACI region proved greater than that expected (see report for Project 1.5.2 & 3) compared to previous successful application of the NHMM in south-west Western Australia (Charles et al. 2007) and the Mount Lofty Ranges, South Australia (Charles et al. 2008, Heneker and Cresswell 2008). Timbal et al. (2008), for example, found great consistency when downscaling 11 IPCC 4AR GCMs for SWWA winter rainfall, whereas here there is less consistency. There is also the argument that the large range of GCM uncertainty is an aspect that calls for close assessment, as was undertaken in the Murray–Darling Basin Sustainable Yields Project (CSIRO 2008).

Despite the marked decrease in confidence due to the GCM limitations, there is a general consistency in several aspects of the projected rainfall changes. Overall, the results point to decreased rainfall totals, particularly in winter, which, combined with the intensity changes for all but the extreme events and increased length of dry spells, suggests that runoff and streamflow responses might be significant.

An important, and potentially confounding, issue is the limitation imposed by having only one projection per GCM and scenario, rather than multiple ensemble members. Thus, the decadal variability of the respective GCMs can have a large influence on the comparisons between periods. Ideally, we would like to have several current and future GCM runs for each GCM and scenario if we are to better understand natural variability in relation to long-term change.

Summary of methods and modifications (with reasons)

Stochastically downscaled multi-site daily rainfall projections were assessed for changes to the following hydrologically relevant metrics:

- Annual rainfall
- Summer (Nov–Mar) and winter (Apr–Oct) rainfall
- Monthly distribution of rainfall
- Maximum daily rainfall
- 90th, 95th, and 99th percentile of daily rainfall
- Number of dry and wet days (wet day is ≥ 1.0 mm)
- Number of consecutive dry and wet days.

The projections were produced by stochastically downscaling an ensemble of multiple GCMs, emissions scenarios, and periods using the Nonhomogeneous hidden Markov model (NHMM, Hughes et al. 1999, Charles et al. 1999). Four GCMs were used, three of which were coupled models as used in the Intergovernmental Panel on Climate Change's Fourth Assessment Report (IPCC AR4): CSIRO Mk3.5 (Australia), GFDL CM2.0 (USA), and MRI CGCM2.3.2a (Japan). The fourth was the CSIRO CCAM atmospheric model that used far-field 'nudging' and sea-surface temperatures from a Mk3.0 run. CCAM is a variable-grid model that is run over Australia at a finer horizontal resolution.

IPCC Scenarios A1B, A2, and B1 were used in this study (mid, high, and low emissions trajectories respectively), although they do not represent the full range of possible climate change. These are the standard emission scenarios used in AR4. Projections were produced for 20-year periods for the middle (2046–2065) and end (2081–2100) of the century. These are the IPCC standard periods for which data are available for all the IPCC AR4 GCMs.

For each of the 24 ensemble members (4 GCMs × 3 emission scenarios × 2 periods) the NHMM was driven by the extracted atmospheric predictors to generate 100 realisations of multi-site daily rainfall for the 30 stations. These projected series were assessed for relative uncertainties and consistencies between the different GCMs, scenarios, and periods.

Summary of links to other projects

The results of this project can be compared to those obtained from GCM-scale results of Project 2.1.5a, the dynamically downscaled results of Projects 2.1.5b,c and 2.3.1, and the projections produced by Project 2.2.3.

Since this is the final project within the current phase of SEACI, as well as reviewing the research completed (as presented here), it is also important to look to the future. This project has produced a large data base of multi-site daily rainfall projections for mid- and end of century. The stochastic nature of the NHMM allowed generation of multiple realisations of multi-site daily rainfall series conditional on the GCM projected atmospheric predictor series. Thus 100 realisations for the four GCMs (CCAM, GFDL,

Mk3.5, MRI) for 20th Century (1961–2000) and three IPCC emissions scenarios (B1 – low; A1B – medium; A2 – high emissions pathways) for mid (2046–2065) and end (2081–2100) of century are available for use in further analysis and applications. An associated eWater project is currently assessing the NHMM results in comparison with several other statistical and dynamical downscaling approaches (Frost et al. 2009).

Testing these NHMM-generated projections as input to hydrological models is now required to determine their adequacy, or otherwise, and to suggest improvements (for example, Charles et al. 2007, Fowler et al. 2007, and Wood et al. 2004 have shown the benefits of statistical downscaling for hydrological applications). NHMM projections have been successfully applied to hydrological modelling investigations of catchment yield changes in the South-West of WA (Berti et al. 2004, Kitsios et al. 2006) and South Australia (Charles et al. 2008, Heneker and Cresswell 2008). Such investigations in the Murray–Darling Basin, using the projections generated in this project, are planned for selected catchments using the SIMHYD hydrological model (Chiew et al. 2002).

Publications arising from this project

Charles, S.P. and Fu, G. (2008). Stochastic downscaling for regional precipitation projections. Proceedings, *HydroPredict'2008*, 15–18 September 2008, Prague, Czech Republic, pp. 269–272.

Frost, A.J, Charles, S.P., Mehrotra, R., Timbal, B., Nguyen, K.C., Chiew, F.H.S., Fu, G., Chandler, R.E., McGregor, J., Kirono, D., Fernandez, E., and Kent, D. (2009). A comparison of multi-site daily rainfall downscaling techniques under Australian conditions (in preparation)

Acknowledgement

This research has been funded by SEACI. A downscaling intercomparison study, funded by the eWater CRC, has improved and extended this research, benefiting the work. The significant efforts of Andrew Frost (Australian Bureau of Meteorology) and the guidance of Francis Chiew (CSIRO) for this downscaling intercomparison study are acknowledged.

References

Berti, M., Bari, M., Charles, S., and Hauck, E. (2004). *Climate change, catchment runoff and risks to water supply in the south-west of Western Australia*. East Perth, Western Australia: Department of Environment. 114 pp.

Charles, S.P., Bates, B.C., and Hughes J.P. (1999). A spatio-temporal model for downscaling precipitation occurrence and amounts. *Journal of Geophysical Research – Atmospheres* 104(D24): 31657–31669.

Charles, S.P., Bari, M.A., Kitsios, A., and Bates, B.C. (2007). Effect of GCM bias on downscaled precipitation and runoff projections for the Serpentine catchment, Western Australia. *International Journal of Climatology* 27: 1673–1690.

Charles, S.P., Heneker, T.M., and Bates, B.C. (2008). Stochastically downscaled rainfall projections and modelled hydrological response for the Mount Lofty Ranges, South Australia. Proceedings *Water Down Under 2008*, Engineers Australia, Adelaide, April 2008, pp. 428–439.

Chiew F.H.S., Peel M.C., and Western A.W. (2002). Application and testing of the simple rainfall–runoff model SIMHYD. In: *Mathematical Models of Small Watershed Hydrology and Applications* (ed. V.P. Singh and D.K. Frevert), Water Resources Publication, Littleton, Colorado, pp. 335–367.

CSIRO (2008). Water availability in the Murray–Darling Basin. A report to the Australian Government from the CSIRO Murray–Darling Basin Sustainable Yields Project. CSIRO Australia, 67 pp.

Fowler, H.J., Blenkinsop, S., and Tebaldi, C. (2007). Linking climate change modelling to impacts studies: recent advances in downscaling techniques for hydrological modelling. *International Journal of Climatology* 27: 1547–1578.

Heneker, T.M. and Cresswell, D. (2008). Potential Impact on Water Resource Availability in the Mount Lofty Ranges due to Climate Change. DWLBC Report 2008/xx (*under review*). Department of Water, Land and Biodiversity Conservation, Government of South Australia. 63 pp.

Hughes. J.P., Guttorp P., and Charles, S.P. (1999). A non-homogeneous hidden Markov model for precipitation occurrence. *Applied Statistics* 48: 15–30.

IPCC (2007). *Climate Change 2007: The Physical Science Basis. Contribution of Working Group I to the Fourth Assessment Report of the Intergovernmental Panel on Climate Change,* ed. Solomon, S., Qin, D., Manning,M., Chen, Z., Marquis, M., Averyt, K.B., Tignor, M., and Miller, H.L. Cambridge University Press, Cambridge, U.K. 996 pp.

Kay, A.L., Davies, H.N., Bell, V.A., and Jones, R.G. (2009). Comparison of uncertainty sources for climate change impacts: flood frequency in England. *Climatic Change* 92: 41–63.

Kitsios A, Bari M.A., and Charles S.P. (2006). *Projected streamflow reduction in Serpentine catchment Western Australia: downscaling from multiple GCMs*. Department of Water, Perth, Australia, 77 pp.

Pitman, A.J. and Perkins, S.E. (2008). Regional projections of future seasonal and annual changes in rainfall and temperature over Australia based on skill-selected AR4 models. *Earth Interactions* 12: 1–50.

Timbal, B., Hope, P., and Charles, S. (2008). Evaluating the consistency between statistically downscaled and global dynamical model climate change projections. *Journal of Climate* 21: 6052–6059.

Wood, A.W., Leung, L.R., Sridhar, V., and Lettenmaier, D.P. (2004). Hydrological implications of dynamical and statistical approaches to downscaling climate model outputs. *Climatic Change* 62: 189–216.

Project Milestone Reporting Table

To be completed prior to commencing the project				Completed at each Milestone date	
Milestone description[1]	Performance indicators[2]	Completion date[3]	Budget[4] for Milestone ($) (SEACI contribution)	Progress[5]	Recommended changes to workplan[6]
1. Determine metrics for assessment that have hydrological relevance	• Metrics selected in consultation with other researchers • Codes developed to calculate and visualise selected metrics	30/06/08		Completed	N/A
2. Compare and assess the properties of the statistically downscaled projections	• Apply metrics to multi-model, multi-scenario, multi-period downscaled projections • Write report summarising findings (10 pages)	31/12/08		Completed (this report)	N/A

APPENDIX A. PROJECTED WEATHER-STATE FREQUENCIES

Table A1. Summer CCAM downscaled weather-state mean frequencies (and standard errors, in brackets, relative to 20C3M)

State	20C3M	A1B mid*	A1B end*	A2 mid	A2 end
1	0.548	0.551 (0.18)	0.552 (0.20)	0.536 (0.45)	0.555 (0.30)
2	0.046	0.047 (0.18)	0.045 (0.18)	0.048 (0.16)	0.046 (0.02)
3	0.088	0.091 (0.35)	0.089 (0.09)	0.093 (0.46)	0.097 (0.95)
4	0.064	0.064 (0.09)	0.067 (1.09)	0.066 (0.63)	0.066 (0.70)
5	0.254	0.247 (0.62)	0.248 (0.61)	0.258 (0.37)	0.235 (1.67)

* 'mid' refers to the 2046–2065 period; 'end' refers to the 2081–2100 period

Table A2. Winter CCAM downscaled weather-state mean frequencies (and standard errors, in brackets, relative to 20C3M)

State	20C3M	A1B mid	A1B end	A2 mid	A2 end
1	0.449	0.480 (2.27)	0.483 (2.48)	0.475 (5.25)	0.451 (0.27)
2	0.100	0.087 (1.96)	0.091 (1.74)	0.091 (4.22)	0.099 (0.65)
3	0.114	0.099 (2.81)	0.103 (1.83)	0.106 (2.92)	0.116 (0.64)
4	0.218	0.213 (0.84)	0.216 (0.36)	0.214 (1.62)	0.218 (0.14)
5	0.118	0.120 (0.30)	0.107 (2.23)	0.114 (1.63)	0.117 (0.66)

Table A3. Summer GFDL downscaled weather-state mean frequencies (and standard errors, in brackets, relative to 20C3M)

State	20C3M	A1B mid	A1B end	A2 mid	A2 end	B1 mid	B1 end
1	0.543	0.602 (2.90)	0.659 (5.42)	0.629 (4.16)	0.629 (4.05)	0.591 (2.42)	0.620 (3.48)
2	0.064	0.047 (2.20)	0.036 (3.83)	0.037 (3.78)	0.040 (3.92)	0.050 (2.13)	0.041 (2.98)
3	0.087	0.072 (2.58)	0.057 (5.01)	0.064 (3.45)	0.064 (3.88)	0.075 (2.36)	0.066 (3.43)
4	0.069	0.072 (0.53)	0.069 (0.16)	0.072 (0.78)	0.067 (0.65)	0.076 (1.30)	0.071 (0.37)
5	0.237	0.208 (2.47)	0.180 (4.56)	0.197 (3.77)	0.200 (2.91)	0.209 (2.29)	0.203 (2.61)

Table A4. Winter GFDL downscaled weather-state mean frequencies (and standard errors, in brackets, relative to 20C3M)

State	20C3M	A1B mid	A1B end	A2 mid	A2 end	B1 mid	B1 end
1	0.439	0.529 (5.30)	0.549 (6.08)	0.487 (2.52)	0.582 (8.58)	0.472 (1.48)	0.498 (2.72)
2	0.088	0.065 (3.79)	0.063 (4.06)	0.076 (1.92)	0.054 (5.96)	0.081 (0.81)	0.072 (2.17)
3	0.126	0.094 (4.07)	0.092 (3.92)	0.111 (1.54)	0.072 (7.53)	0.119 (0.58)	0.105 (2.05)
4	0.219	0.207 (1.38)	0.209 (1.03)	0.223 (0.58)	0.201 (2.05)	0.227 (0.90)	0.215 (0.43)
5	0.129	0.106 (2.82)	0.087 (6.05)	0.103 (3.52)	0.091 (5.52)	0.101 (3.39)	0.111 (2.61)

Table A5. Summer Mk3.5 downscaled weather-state mean frequencies (and standard errors, in brackets, relative to 20C3M)

State	20C3M	A1B mid	A1B end	A2 mid	A2 end	B1 mid	B1 end
1	0.525	0.556 (1.67)	0.565 (1.95)	0.573 (2.21)	0.578 (2.75)	0.569 (2.05)	0.533 (0.41)
2	0.083	0.068 (1.49)	0.055 (3.07)	0.058 (2.67)	0.051 (3.73)	0.058 (2.80)	0.070 (1.46)
3	0.100	0.095 (0.73)	0.089 (1.72)	0.084 (2.11)	0.085 (2.32)	0.087 (2.04)	0.099 (0.19)
4	0.055	0.063 (2.81)	0.064 (3.22)	0.062 (2.13)	0.068 (4.17)	0.062 (2.35)	0.062 (3.09)
5	0.237	0.218 (2.12)	0.227 (0.92)	0.223 (1.30)	0.219 (1.74)	0.224 (1.08)	0.236 (0.06)

Table A6. Winter Mk3.5 downscaled weather-state mean frequencies (and standard errors, in brackets, relative to 20C3M)

State	20C3M	A1B mid	A1B end	A2 mid	A2 end	B1 mid	B1 end
1	0.439	0.512 (3.45)	0.550 (5.26)	0.495 (2.60)	0.562 (6.09)	0.488 (2.40)	0.513 (3.89)
2	0.117	0.089 (2.81)	0.067 (4.95)	0.093 (2.09)	0.063 (5.74)	0.091 (2.61)	0.087 (2.87)
3	0.098	0.083 (2.48)	0.071 (4.22)	0.085 (2.08)	0.069 (4.50)	0.087 (1.51)	0.083 (2.55)
4	0.206	0.200 (0.65)	0.201 (0.45)	0.214 (1.11)	0.199 (0.79)	0.208 (0.24)	0.208 (0.23)
5	0.140	0.116 (2.64)	0.111 (3.53)	0.113 (3.11)	0.107 (4.06)	0.126 (1.49)	0.108 (3.59)

Table A7. Summer MRI downscaled weather-state mean frequencies (and standard errors, in brackets, relative to 20C3M)

State	20C3M	A1B mid	A1B end	A2 mid	A2 end	B1 mid	B1 end
1	0.561	0.584 (1.01)	0.553 (0.31)	0.549 (0.53)	0.590 (1.24)	0.564 (0.16)	0.549 (0.56)
2	0.051	0.040 (1.44)	0.054 (0.43)	0.052 (0.13)	0.041 (1.49)	0.047 (0.52)	0.052 (0.16)
3	0.081	0.073 (1.07)	0.085 (0.43)	0.083 (0.21)	0.072 (1.28)	0.082 (0.10)	0.083 (0.18)
4	0.067	0.071 (0.96)	0.069 (0.30)	0.070 (0.66)	0.067 (0.10)	0.064 (1.08)	0.064 (0.97)
5	0.239	0.231 (0.60)	0.239 (0.05)	0.246 (0.64)	0.230 (0.72)	0.242 (0.23)	0.252 (1.10)

Table A8. Winter MRI downscaled weather-state mean frequencies (and standard errors, in brackets, relative to 20C3M)

State	20C3M	A1B mid	A1B end	A2 mid	A2 end	B1 mid	B1 end
1	0.450	0.514 (3.36)	0.534 (4.20)	0.503 (2.86)	0.541 (4.11)	0.506 (2.71)	0.509 (2.85)
2	0.104	0.083 (2.38)	0.083 (2.99)	0.088 (1.73)	0.082 (2.40)	0.083 (2.89)	0.089 (1.70)
3	0.127	0.105 (2.03)	0.091 (3.97)	0.111 (1.49)	0.094 (3.10)	0.105 (2.27)	0.103 (2.63)
4	0.206	0.202 (0.45)	0.196 (1.03)	0.202 (0.51)	0.190 (1.98)	0.202 (0.47)	0.211 (0.51)
5	0.113	0.095 (2.26)	0.096 (2.28)	0.096 (2.44)	0.093 (3.16)	0.105 (0.97)	0.087 (3.51)

APPENDIX B. Table B1. Range in mean annual percentage rainfall change by GCM and by scenario for 2046–2065 (left) and 2081–2100 (right)

Station	B1	A1B	A2	CCAM	GFDL	Mk3.5	MRI	B1	A1B	A2	CCAM	GFDL	Mk3.5	MRI
1	9.08	12.71	17.21	2.30	2.40	4.79	13.71	10.71	25.56	28.43	7.18	4.87	7.31	12.54
2	9.81	10.81	16.26	3.21	5.58	2.90	10.37	8.51	19.00	22.23	2.25	6.38	7.39	7.87
3	8.56	11.74	13.02	1.60	5.89	2.35	9.96	8.71	19.61	22.04	1.12	8.04	9.78	7.71
4	10.93	11.19	17.24	3.00	3.74	4.05	10.15	11.27	22.21	20.54	1.94	8.01	7.87	8.42
5	10.10	10.95	14.08	2.58	6.11	3.44	11.12	10.71	23.69	27.36	4.26	4.91	8.59	9.33
6	9.41	10.44	13.43	1.48	6.50	3.36	9.69	8.63	22.05	24.96	1.64	7.20	11.28	7.58
7	9.56	11.76	12.88	1.07	6.69	3.90	9.99	9.03	22.70	25.97	2.38	6.80	10.11	9.74
8	11.45	12.65	16.12	1.69	3.90	5.02	12.91	12.49	25.16	28.01	2.01	5.75	9.29	11.03
9	9.72	12.03	14.18	1.55	7.68	2.27	10.40	9.97	23.16	25.43	0.91	10.15	11.45	7.90
10	8.91	11.66	14.51	2.02	5.99	2.24	8.71	10.01	20.44	23.09	2.17	6.43	8.76	7.52
11	10.49	13.51	17.86	4.23	6.80	4.12	12.54	11.46	25.25	29.58	2.82	8.75	12.25	11.04
12	10.69	13.48	16.78	3.80	4.38	6.61	13.24	10.32	23.35	27.45	5.65	4.33	8.49	10.23
13	11.94	13.80	16.43	2.58	3.31	4.46	13.63	14.35	28.62	29.66	2.72	4.27	9.47	13.07
14	13.94	15.84	21.29	3.73	5.49	5.92	12.86	12.56	28.40	30.70	3.70	6.76	10.88	13.56
15	8.52	13.67	17.14	2.83	6.33	3.88	12.60	11.84	24.67	30.57	4.07	5.55	12.21	10.70
16	9.93	14.56	19.10	4.31	2.08	5.55	13.38	11.83	26.00	30.30	4.96	6.18	7.90	12.86
17	10.10	10.84	13.60	1.79	5.82	2.60	10.06	9.51	22.61	28.33	4.42	5.41	9.95	9.58
18	10.61	13.32	16.94	2.72	3.88	3.40	12.48	12.57	26.43	27.70	3.39	3.74	8.76	12.44
19	11.23	12.93	14.37	2.06	7.58	3.55	10.89	10.37	24.93	28.92	2.26	7.67	11.49	7.28
20	10.72	11.05	12.23	1.75	7.71	4.62	10.44	9.16	23.20	28.42	4.44	5.40	10.60	8.97
21	10.14	12.61	14.33	2.62	8.30	3.48	10.24	8.13	22.34	27.73	3.94	8.75	12.67	8.11
22	11.46	12.46	14.17	1.33	8.36	3.58	10.69	9.77	24.13	28.54	4.12	7.84	10.12	8.02
23	10.62	12.01	13.67	1.47	8.35	2.92	11.33	10.00	23.18	27.20	2.81	6.53	11.45	8.12
24	9.50	10.12	10.83	1.62	8.44	2.56	8.95	7.95	20.40	24.13	2.20	9.29	11.98	6.77
25	7.71	10.73	8.67	1.10	9.25	1.62	8.72	7.09	18.73	22.12	1.06	10.60	12.16	6.68
26	8.86	10.99	12.71	0.91	5.00	2.85	10.26	10.30	17.94	18.73	0.84	5.44	10.50	7.96
27	8.89	9.04	8.96	2.07	8.43	2.62	8.01	6.69	17.68	20.89	2.97	4.74	7.88	5.26
28	8.15	11.94	8.41	0.30	10.55	1.43	7.96	8.34	19.26	22.17	0.36	11.22	13.14	7.93

29	8.81	9.85	7.56	0.93	10.14	1.89	7.66	7.10	18.72	21.13	1.02	10.09	11.87	6.77
30	6.49	12.60	11.07	1.78	9.29	0.55	5.69	7.77	18.51	20.82	0.64	11.35	11.39	6.90